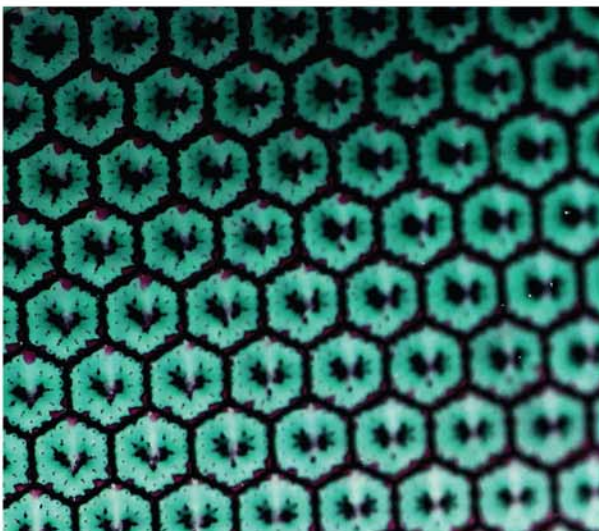
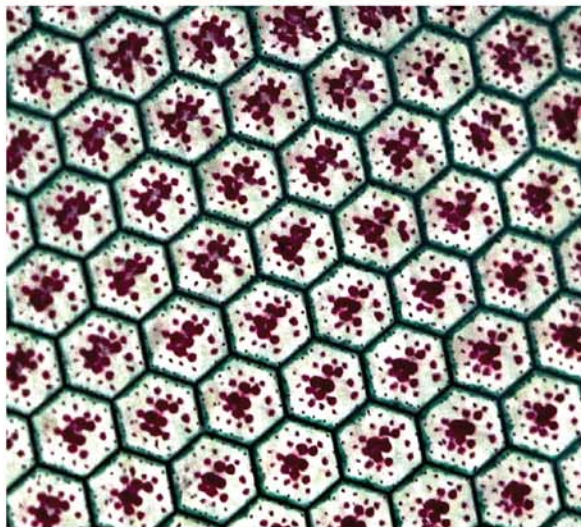
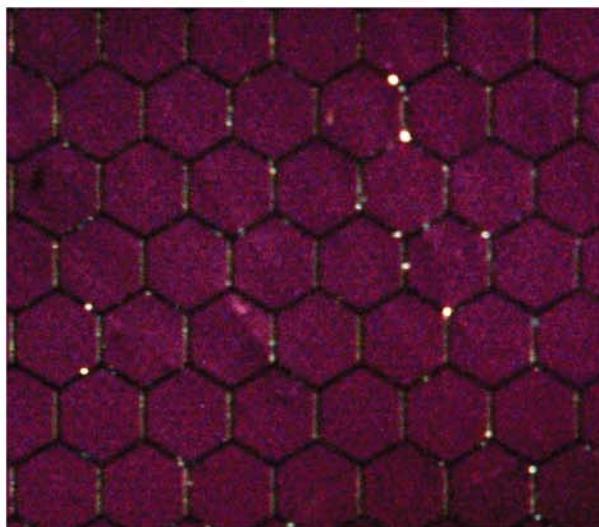


Volume 54 • Issue 17 | June 10, 2015

applied optics

APPLICATIONS-CENTERED RESEARCH IN OPTICS



OSA[®]
The Optical Society



INTERNATIONAL
YEAR OF LIGHT
2015

ISSN: 1559-128X

ao.osa.org

Electrokinetic pixels with biprimary inks for color displays and color-temperature-tunable smart windows

S. MUKHERJEE,¹ W. L. HSIEH,³ N. SMITH,² M. GOULDING,² AND J. HEIKENFELD^{1,*}

¹Department of Electrical Engineering and Computing Systems, University of Cincinnati, Cincinnati, Ohio 45221, USA

²Merck Chemicals Ltd., Chilworth Technical Centre, Southampton, Hampshire SO16 7QD, UK

³Institute of Applied Mechanics, National Taiwan University, Taipei 106, Taiwan

*Corresponding author: heikenjc@ucmail.uc.edu

Received 11 March 2015; revised 5 May 2015; accepted 11 May 2015; posted 18 May 2015 (Doc. ID 235176); published 10 June 2015

We report on the advanced implementation of the biprimary color system in applications where subtractive color is performed inside a single pixel to alter the magnitude and color of reflection (electronic paper displays) or the optical transmission and color temperature (smart windows). A novel device structure can switch between four states: clear, black, either of two complementary colors from RGB and CMY sets, and also mixed states between one of these four states. The device structure utilizes an electrokinetic pixel structure, which combines the spectral performance of in-plane electrophoretic devices with the improved switching speeds of vertical electrophoresis. The electrophoretic dispersions are dual-particle dual-colored and are controlled using two traditional planar electrokinetic electrodes on the front and back substrates, along with a third electrode conveniently located at the perimeter of each unit cell. Demonstrated performance includes contrast ratios reaching $\sim 10:1$, reflectance of $\sim 62\%$, and transparency of $\sim 75\%$. For electronic paper displays, these results provide a pathway to double the reflective performance compared to the traditional RGBW color-filter approach. For smart windows, the technology provides not only control of shade (transmission) but also provides complete control over color temperature. Furthermore, this three-electrode device can be roll-to-roll fabricated without need for any alignment steps, requiring only a single micro-replication step followed by self-aligned contact printing of the third electrode. © 2015 Optical Society of America

OCIS codes: (120.2040) Displays; (130.7408) Wavelength filtering devices; (120.0280) Remote sensing and sensors; (130.4815) Optical switching devices.

<http://dx.doi.org/10.1364/AO.54.005603>

1. INTRODUCTION

Light valves used in displays [1–3] or in smart windows [4,5] are typically limited to electronic switching between two states, typically a clear and a black state. For full-color operation, color filters are utilized and typically reduce the optical transmission or reflection by $3\times$ [6]. Furthermore, even the clear to opaque switching mechanism can be inefficient itself, further limiting the optical performance to the point of preventing commercial success for applications such as color reflective displays (e-Paper) [6].

Our research group previously proposed a new biprimary color system [7] and recently demonstrated basic proof of principle using traditional in-plane electrophoretic display architecture [8,9]. The biprimary color system uniquely allows a single pixel to be switched through mixtures of color states of K (black), W (white), and X and X', where X and X' states are the two complementary colors from the RGB and CMY

primaries (e.g., R/C, G/M, or B/Y). As demonstrated [7], the performance doubles the reflectance and color saturation for reflective e-Paper displays [6]. However, several significant drawbacks still exist from an applied perspective. First, in-plane [9] electrophoresis is slow due to long path lengths. Second, the need for at least three electrode controls is complex and difficult to reliably fabricate, especially when low-cost and large-area devices are required.

Here, we report electrokinetic pixels with biprimary inks, resolving several of the previous challenges in the use of biprimary color. The device structure utilizes an advanced electrokinetic pixel structure, which, for biprimary color-to-color switching states, combines the spectral performance of in-plane electrophoretic devices with the improved switching speeds of vertical electrophoresis [10–12]. The electrophoretic dispersions are dual-particle, dual-colored [13], and are controlled using two planar electrokinetic electrodes on the front and back

substrates, along with a new third electrode provided at the perimeter of each unit cell. Demonstrated performance includes contrast ratios up to $\sim 10:1$, reflectance of $\sim 62\%$, and transparency of $\sim 75\%$. For electronic paper displays, these results provide a pathway to double the reflective and color-fraction performance [6] compared to traditional color-filter approaches. Because switching speeds are not fast (seconds to 10^3 's of seconds), signage is the most likely e-Paper application [6].

We have further identified that, with a single biprimary ink dispersion such as B/Y, this simple single-layer technology provides previously undemonstrated capability for smart windows. Not only can optical transmission be shaded, but, uniquely, complete control over color-temperature is provided. This control over color temperature is a significant value addition for windows as a source of external light, mirroring the value already existing in color temperature for light bulbs, and providing value that does not exist in mechanical shading. Especially important for large-area applications such as windows, the three-electrode device can be roll-to-roll fabricated without the need for any alignment, requiring only a single micro-replication step followed by self-aligned contact printing of the third electrode. Furthermore, this approach is likely easily extendable to independent control of privacy/shade and of visible/infrared transmission.

2. DEVICE DESIGN, FABRICATION, AND MATERIALS

Figure 1 shows the top view of the devices and the cross-sectional view of two variations of the device construction, each of which function identically. The device uses electrophoresis to attract charged colored particles to the top $\text{In}_2\text{O}_3:\text{SnO}_2$ (ITO) transparent electrode (spread to display their color), or to compact (hide) them inside the pits adjacent to the bottom ITO transparent electrode, or compact them at the hexagonal metal electrode found along the perimeter of cell.

The tested devices were fabricated on 2 in. \times 2 in. aluminosilicate glass substrates with a net active area of 1.6 in. \times 1.6 in. The devices were filled with dual-color, dual-particle colloidal dispersion inks supplied by Merck Chemicals Ltd. [13], by placing a droplet of the dispersion in the center of a first substrate, and then clamping the second substrate to the first with binder clips. The particles are polydisperse, such that their electrophoretic mobilities are dissimilar but around $5 \times 10^{-6} \text{ cm}^2/\text{V}\cdot\text{s}$, as previously reported [8]. Differing mobilities lead to different velocities and, therefore, allow incomplete transport (spreading) of the particles if the application of voltage is limited in time. The importance of this spreading will be presented in the next section on device operation. The raw spectral properties of the colloidal dispersion inks themselves, measured external to a device, can also be found in our previous work [8]. Both transmissive and reflective devices were created and tested in this work. The as-fabricated device is inherently transmissive mode. For the reflective mode, placed behind the device was a 3M ESR reflector film coated with a diffuse barium sulfate powder, resulting in a $>96\%$ Lambertian reflectance. Because this reflector is decoupled from the device (air gap), there are no issues with light-out coupling due to

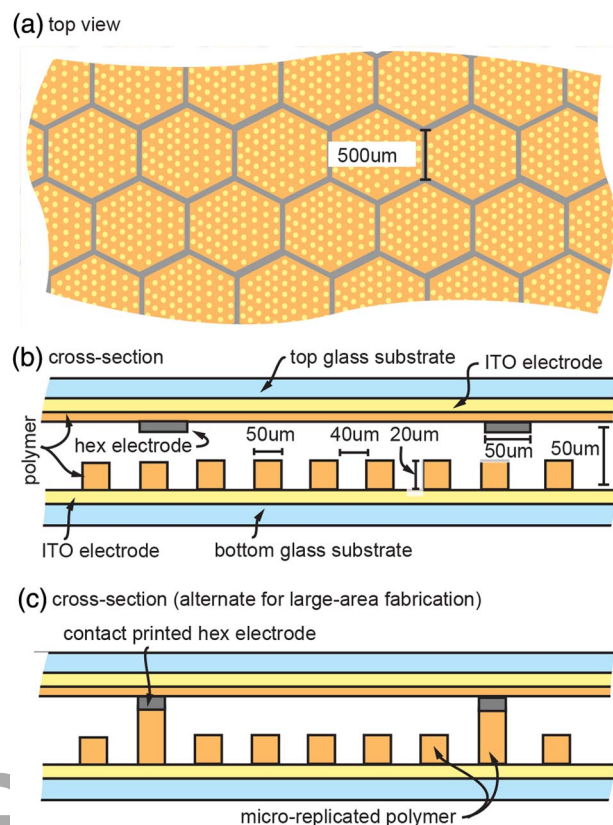


Fig. 1. Diagrams of device construction with dimensions including a (a) top view and (b),(c) cross-sectional views of two different methods of fabrication where (c) can be potentially made roll-to-roll without any alignment steps. Note, the device is shown without filling of the electrophoretic ink dispersion.

total-internal reflection [14], and the expected reflectance will, therefore, be roughly the square of the transmittance.

There are two variants of fabrication. The first approach, shown in Fig. 1(b), is useful for research purposes, as the device features are formed using purely conventional photolithographic means [the polymer in Fig. 1(b) is SU-8, which is an electrically insulating negative tone photoresist]. The second approach, shown in Fig. 1(c), is designed for low-cost and highly scalable manufacturing. Hewlett Packard has already shown that the lower micro-replicated polymer can be made using simple roll-to-roll cast and cure technology [10–12]. The raised (higher) cell perimeters can then be coated using simple and proven contact printing (transfer) of a conductive Ag epoxy from a roller coated with the Ag epoxy. The process used for Fig. 1(c) is highly attractive because the entire process can be implemented roll-to-roll and requires no alignment. In addition, the Ag epoxy can also be used to provide a closed-cell seal to prevent pigment particle movement from cell to cell, which is important for applications such as windows where gravity could cause a net pigment particle migration due to gravity. Further supporting the simplicity of fabrication, unlike our previous in-plane designs [8], the hexagonal electrode grid is highly fault tolerant through electrical path redundancy (open-circuit defects in the lines are a nonissue). The only meaningful differences between the design of Figs. 1(b) and 1(c), is that

(1) Fig. 1(b) is more likely capable of higher-resolution features, which are important for displays; (2) Fig. 1(b) requires additional channel height spacers (not shown); (3) the hexagonal electrode of Fig. 1(b) has more exposed surface area to support compaction (greater hiding) of charged colored particles on it. The device of Fig. 1(b) was utilized for the research results shown herein.

3. GENERAL PHYSICS OF OPERATION

The general physics of operation are now discussed for devices, covering reflective and transmissive modes of operation. The biprimary system for transmissive smart-windows uses only one color set, such as B/Y, and requires no subpixelation. The biprimary system for e-Paper displays utilizes three subpixels, each subpixel having one dual-color, dual-particle ink dispersion of R/C, G/M, or B/Y colors [8]. In each subpixel, the complementary colored particles are oppositely charged, with an example for the G/M subpixel shown in Fig. 2.

For the G/M example shown in Fig. 2, the four states of KWGM are illustrated, including two possible W states. For the experiments reported here, the DC voltages applied to the electrodes are limited to only +25, -25, and 0 V. The sequence of states (KWGM) is shown in the optimal order for the fastest and most complete transitions for the current device geometry and ink dispersions, and other transitions have slower switching speeds or poorer color performance. Generally, switching that compacts a particle first into the pits is the ideal state before the particle is then spread across the top substrate. The transitions themselves are complex spectrally; therefore, online supplementary videos (*Visualization 1* and *Visualization 2*) are provided for the R/C dispersion, showing full cycling through all the colors: $K \rightarrow W \rightarrow R \rightarrow W \rightarrow K$ and $K \rightarrow W \rightarrow C \rightarrow W \rightarrow K$. The videos are real time and include notations of when voltages are changed. The time cycles listed below will be roughly those observed at a distance by the human eye for which online videos have been provided (zoom out). Note, the preliminary inks used here have particles with electrophoretic mobilities that are one order of magnitude lower than the best commercial electrophoretic ink dispersions. Because switching time is proportional to electrophoretic mobility, much faster speeds are possible in future work, as is improved particle color saturation as well. An M/G example for sequential switching through various states is now described in greater detail.

K State: The initial state with no voltage applied is black as the particles spread evenly over time in the absence of voltage. Actively switching to the black state will be described at the end of this section.

W state: Starting from the previous K state, a W state is achieved by setting the bottom ITO electrode to -25 V and the hexagonal electrodes to +25 V, and the top ITO electrode is kept at 0 V. As a result, negatively charged green particles are compacted at the hexagonal electrode and the magenta particles are compacted in the pits. After the switching is adequately complete (~10 s), this state can be maintained with voltages of less than 10 V.

M state: Next, an M state is achieved from the previous W state by switching the bottom ITO electrode to +25 V and the

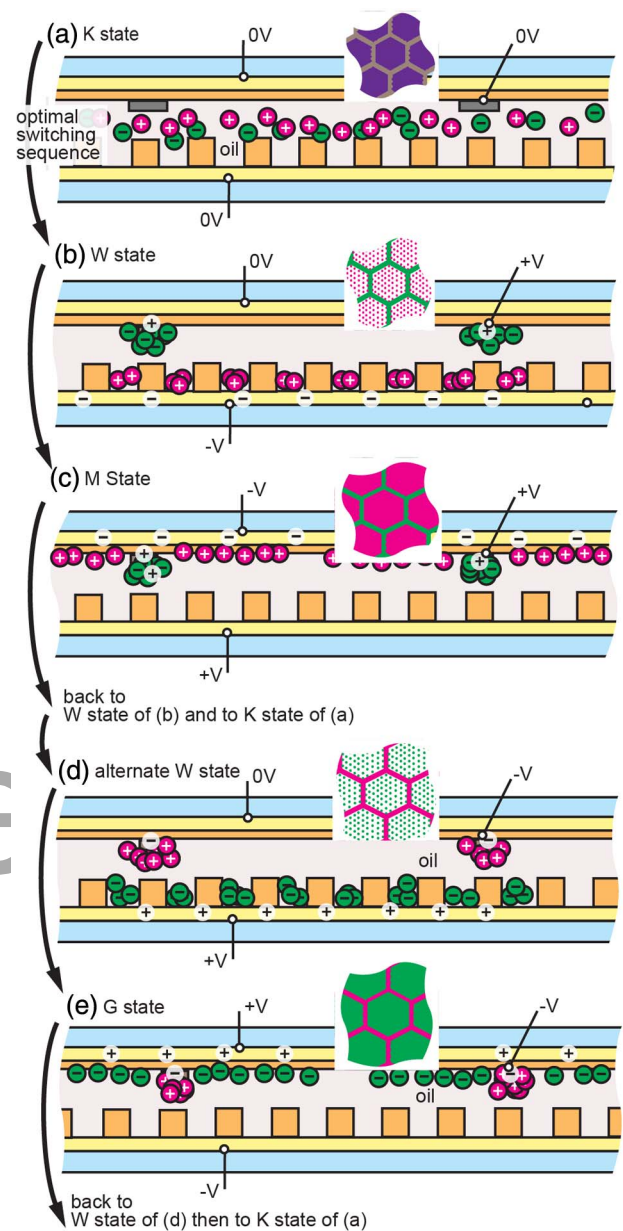


Fig. 2. Device operation in (a) K (black), (b) W (white), (c) M (magenta), (d) alternate W (white), and (e) G (green) states with inset diagrams of the top view. With the current device dimensions and ink dispersions, the sequence shown was found to be optimal for switching between states.

top ITO electrode to -25 V, which then draws the M particles to a spread state on the top plate, while the hexagonal electrode is still maintained at the same +25V from previous state, retaining compaction of the G particles. The switching is complete as perceived by the naked eye at a distance, in (~10 s) and can be maintained at a low holding voltage of ± 10 V.

Alternate W state: The alternate W state is where the negatively charged green particles are compacted in the micropits by setting the bottom electrode to +25 V and compacting the M particles to the hexagonal electrode by setting it to -25 V while keeping the top ITO plate at 0 V. As shown in Fig. 2, for optimal optical performance (most complete particle move-

ment), it is best to leave the M state (2c), return to the original W state (2b), then actively to the K state (see section below), then finally switch to the alternate W state. Again, this state can be maintained at a low holding voltage of ± 10 V.

G state: Next, the G state is set from the previous W state by reversing the bottom ITO plate to -25 V, while the top plate is switched to $+25$ V, which moves and spreads G particles to the top. The hexagonal electrode is kept at the same potential of -25 V from the previous state, which still holds the M particles in their place. This state can then be maintained at a low holding voltage of ± 10 V after the switching is complete in ~ 10 s.

Actively Returning to the K state: A multistep process is needed, which is similar to that needed for the alternate W state, for optimal optical performance (most complete particle movement). It is best to first leave the G state (2e) by returning to the alternate W state (d). Then, the K state can be achieved within ~ 7 s by spreading the particles through repeatedly reversing voltage between the bottom and the hex electrodes (Fig. 1), followed by removing all the voltages. Complete mixing is difficult to quantify and is achieved only after the voltages are removed for 10's of seconds. The reader is again encouraged to view the supplementary online switching videos as a reference (Visualization 1 and Visualization 2).

4. EXPERIMENTAL RESULTS

A. Reflective Results (e-Paper Applications).

Reflective measurements were made utilizing an Ocean Optics HR4000CG-UV-NIR spectrometer. The sample device is illuminated with white light using THORLAB OSL fiber illuminator. The spectrum measured is specular excluded and collected by an Ocean Optics P200-2-VIS-NIR fiber fitted with a 74-VIS collimating lens. The setup is calibrated against Labsphere Spectralon reflection standards of 99% and 2% for bright and dark spectrum, respectively. The reflection spectra of all the KWGM states were measured in the device and plotted in Fig. 3 along with zoom-in photos of the states. The best achievable W state was found to be $\sim 62\%$ reflective with a K state of $\sim 6\%$. The G and M states are much more saturated than that demonstrated for the in-plane structure [8] due to pigment compaction at multiple pits and due to shorter path lengths in moving to the spread state. The colloidal ink dispersions have not been optimized for this particular device structure and, therefore, with such optimization, even better performance is fully expected for color saturation, black state, and white state. Even so, right now, a reflectance of $\sim 62\%$ with biprimary color already provides more than twice the color performance [6] compared to RGBW color filters on e-Ink technology (vertical electrophoresis, $\sim 20\%$ reflectance for white) [6].

B. Transmissive Results (Smart Window Applications)

For transmissive operation, an R/C colloidal dispersion ink was chosen as pictured in Fig. 4 because the other ink dispersions (M/G, Y/B) currently lack the opacity needed for a good black transmissive state. Like the reflective results, optimizing the ink dispersions and/or constructing a thicker channel should im-

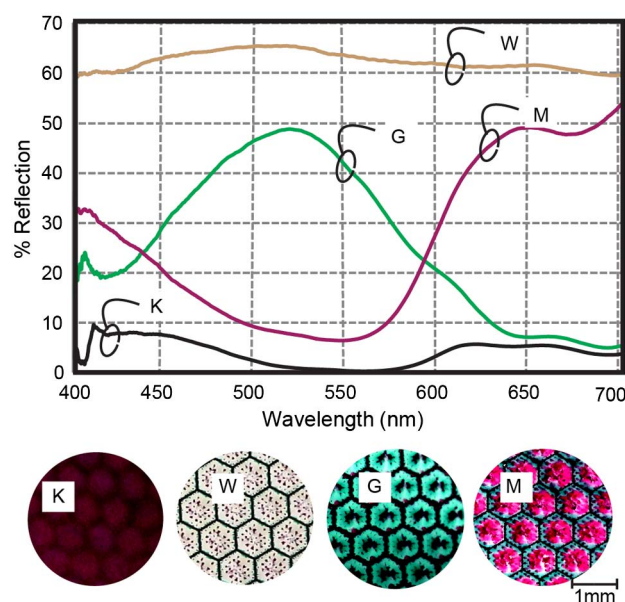


Fig. 3. Reflection spectra of a device with G/M (green/magenta) particle dispersion, along with inset photographs of each state. Data was obtained by placing a 96% diffuse reflector beneath the device structure shown in Fig. 2.

prove the opacity of the black states. The dispersions and device were originally developed for reflective operation, which has twice the optical path length of transmissive mode. Of particular interest for windows is improving the Y/B ink dispersions for transmissive color-temperature control.

Transmission measurements were also made utilizing the Ocean Optics HR4000CG-UV-NIR spectrometer and a fiber illuminator. The incoming transmitted spectrum through the device is collected by an Ocean Optics P200-2-VIS-NIR attached to a 74-VIS collimating lens. The setup is calibrated with respect to air; hence, the transmission spectra include the light absorption and Fresnel reflection due to the stack of the device ($\sim 12\%$ of the incoming light). The transmission spectra

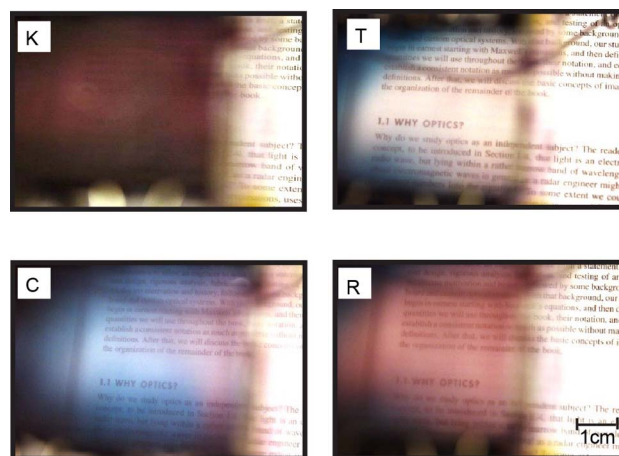


Fig. 4. Zoom-out photographs showing all the KTCR (black/transmissive/cyan/red) states for the RC (red/cyan) dispersion in a transmissive mode device. An optics textbook is provided behind the device to validate clarity of transmission and transmission efficiency.

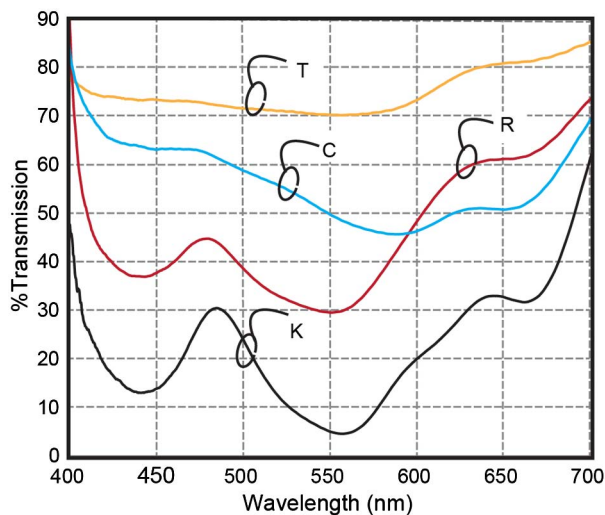


Fig. 5. Transmission spectra of the R/C (red/cyan) dispersion measured in the device for all the KTCR states (black/transmissive/cyan/red).

are shown in Fig. 5 for the four states of K (dimmed), T (clear white), C (cyan), and R (red). The clear white transparent (T) state is found to be $\sim 75\%$, comparable or better than the transparency of other technologies that exists for the smart windows [15,16].

C. Experimental and Modeling Results for Pigment Compaction

To further understand the device operating principles, additional modeling analysis was also performed. One question of particular interest was to determine how charged particles could transition from compaction on the hex borders to an adequately even spreading across the cell or into the micropits across the cell. The optimum switching sequence shown in Fig. 2 was selected because of this very issue, which is now presented here in more detail through supplemental modeling work. A COMSOL model was used to investigate unit cells as shown in Fig. 6(a). The 2D simulation pictures (b)–(e) show the E-field lines (arrows) and the electric potential (color gradient) and, therefore, show the path through which positive particles will move. Conversely, the negative particles will move in the reverse direction toward the arrowheads. The arrows above the hexagonal electrode can be ignored because in the device a solid dielectric is located there.

The simulation result of W state of Fig. 2(b) is shown in Fig. 6(b). The behavior of particles moving from the K state of Fig. 2(a) to the W state of Fig. 2(b) is conventional, and the simulation simply confirms the expected and observed behavior. For switching from the W state of Fig. 2(b) to the M state of Fig. 2(c), the simulation shown in Fig. 6(c) is a simple result and expected.

Now, the transition from the M state of Fig. 2(c) to the alternate W state of Fig. 2(d) is not conventional. For switching it from M to alternate W state, the M pigment needs to move in-plane, which is slow but conventional.

However, the G particles, which were already on the hex electrodes, will move straight down to the nearest pits if one

(a) unit pixel in 3D, red area representing the selected section

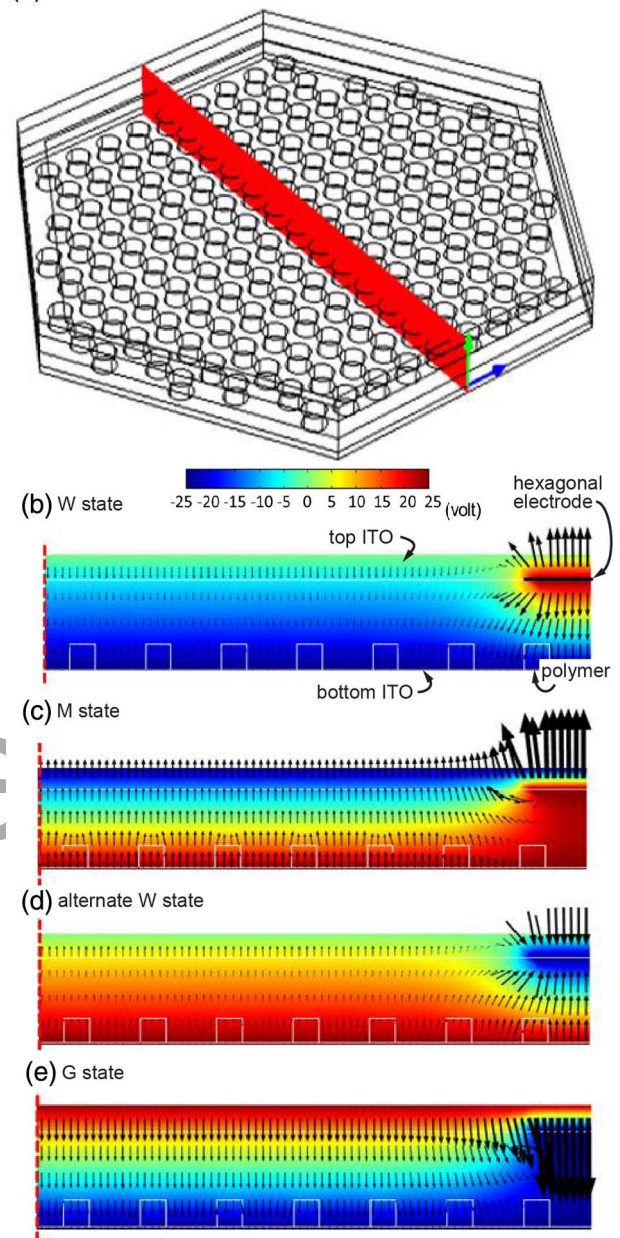


Fig. 6. (a) 3D model of a unit pixel (b)–(e). Simulation results of the states showing the E-field path for W, M, alternate W, and G states.

attempts to go straight from the M state to the alternate W state. This can be seen also as a path of strong E-field, as shown in Fig. 6(d). Hence, intermediate states of switching, as shown in Fig. 2, are necessary to properly spread the G particles and complete the transition to the alternate W state.

Next, from the alternate W state to the G state, the G particles are spread, and the switching is conventional and simple/expected [Fig. 6(e)]. Last, from the G state to the K state, there are similar challenges to that of switching to the alternate W state [Fig. 6(d)], and a multistep switching process is required.

The simulation and above discussion highlight the need for a more optimal arrangement of the micropits. The micropit array is evenly spaced, as designed for a conventional

single-particle electrokinetic display operation. A higher density of the micropits, or larger micropits, toward the perimeter of the pixel would be expected to provide a faster switch to high optical transmission, as the pigment will have a shorter path to travel for compaction after leaving the hex electrode. This and other modifications are possible, such as also optimizing the hexagonal electrode pitch relative to the micropits arrangement, but are beyond the scope of this work. Other possible improvements include use of index-matched ITO and index-matching of the fluids to the surrounding layers and particles (less Fresnel reflection, less scattering), and the significant need for optimization of the particle dispersions themselves.

5. BRIEF DISCUSSION AND MOCK-UP FOR SMART WINDOWS

The application for smart windows is discussed in greater detail, an application where the combination of simple fabrication and increased optical performance is likely most compelling. The most important colloidal dispersion ink for smart windows would be B/Y. Smart windows based on electrochromism [15] or polymer dispersed liquid crystals [16] have struggled to find broad-based commercial success partly because their performance value over traditional mechanical blinds is not significant. Windows are utilized as a form of lighting, and the commercial market has been sensitized for decades to demand lighting with a variety of color temperatures (bluish versus yellowish light). Therefore, the devices demonstrated here, along with an improved B/Y dispersion, could provide the first ever smart window capable of dimming light transmission and fully altering the color temperature of transmitted light. The yellow state could even be amber/orange tinted, which would likely only improve the opacity of the black state.

Figure 7 shows a printed mock-up of this technology, including the optical losses expected by use of conventional pigment particles, due to factoring in loss expected for the area of the micropits and hexagonal electrodes. The mock-up shows a

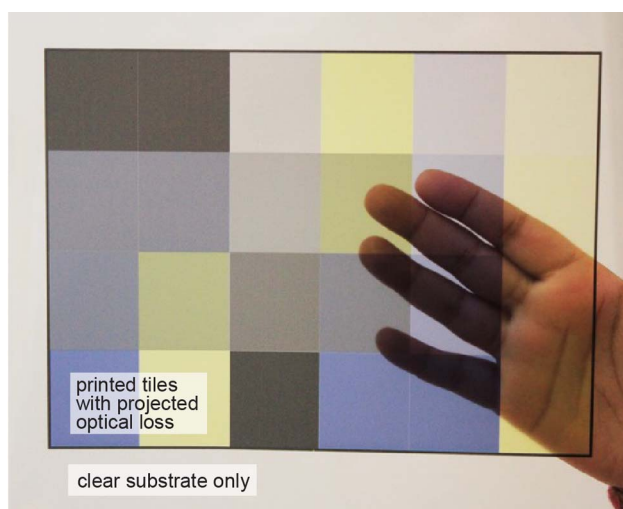


Fig. 7. Blue/yellow printed mock-up of the window application, the colors showing blue, yellow, gray, and all the intermediate shades. The mock-up includes the expected optical loss due to pixel borders and micropits.

variety of clear, black, gray, and color-temperature modified states. More detailed spectral measurements of actual blue and yellow particle dispersions can be found in our previous work [8].

Last, it should also be noted that, with other types of two particle dispersions, windows could be potentially created with independent control of shade and privacy (black particles and white scattering particles) or independent thermal control (black particle, clear but IR absorbing particle). In fact, high-performance two-particle dispersions such as black/white are easier to create because the particles are chemically distinct from each other on their surface and are readily available commercially (e.g., used in E-Ink technology). These black/white particle dispersions have $\sim 10\times$ higher electrophoretic mobility than the dispersions used here and excellent long-life stability.

6. CONCLUSION

We have successfully demonstrated a new three-electrode electrokinetic device structure with dual-particle, dual-color colloidal dispersion inks for reflective E-paper displays and smart windows. This device adds the ability of switching pixels into multiple spectral states, potentially improving color performance in reflective displays and providing color temperature control for smart windows. The switching speeds are on the order of 10 s or more, likely relegating e-Paper used to signage applications. For smart windows, these speeds are similar to those commercially found in electrochromic windows. The results shown herein already show a significant boost in transmission, reflection, and color performance, despite the fact that the dual-particle dual-color dispersions are far from optimized performance, nor has the device structure been optimized. In addition, the devices involve very few and simple fabrication steps, such that low-cost and large area fabrication is quite feasible. Of all the device aspects, particle dispersion improvements are likely most critical, especially in the areas of spectral properties, switching speed, and particle/dispersion stability.

National Science Foundation (NSF) (1231668).

The Cincinnati authors would like to thank Philip Schultz, Alex Schultz, Daniel Rose, and Zachary Sonner for providing valuable assistance in sample fabrication and characterization. The authors would also like to thank members Dr. Laura Kramer and Dr. Qin Liu from the Hewlett Packard Research center, Corvallis, Oregon, for assistance in electrokinetic device development.

See Visualization 1 and Visualization 2 for supporting content.

REFERENCES

1. Y. Najjoh, T. Yashiro, S. Hirano, Y. Okada, S. Kim, H. Takahashi, K. Fujimura, and H. Kondoh, "Multilayered electrochromic display," in *proceedings of IDW*, (ITE and SID, 2011), pp. 375–378, www.rioh.com
2. R. A. Hayes and B. J. Feenstra, "Video-speed electronic paper based on electrowetting," *Nature* **425**, 383–385 (2003).
3. B. Comiskey, J. D. Albert, H. Yoshizawa, and J. Jacobson, "An electrophoretic ink for all printed reflective electronic displays," *Nature* **394**, 253–255 (1998).
4. R. Baetens, B. Jelle, and A. Gustavsen, "Properties, requirements and possibilities of smart windows for dynamic daylight and solar energy

- control in buildings: a state-of-the-art review," *Sol. Energy Mater. Sol. Cells* **94**, 87–105 (2010).
5. H. You and A. Steckl, "Versatile electrowetting arrays for smart window applications from small to large pixels on fixed and flexible substrates," *Sol. Energy Mater. Sol. Cells* **117**, 544–548 (2013).
 6. J. Heikenfeld, P. Drzaic, J. S. Yeo, and T. Koch, "Review paper: a critical review of the present and future prospects for electronic paper," *J. Soc. Inf. Disp.* **19**, 129–156 (2011).
 7. J. Heikenfeld, "A new biprimary color system for doubling the reflectance and colorfulness of E-paper," *Proc. SPIE* **7956**, 1–6 (2011).
 8. S. Mukherjee, N. Smith, M. Goulding, Q. Liu, L. Kramer, S. Kularatne, and J. Heikenfeld, "A first demonstration and analysis of the biprimary color system for reflective displays," *J. Soc. Inf. Disp.* **22**, 106–114 (2014).
 9. K. H. Lenssen, P. Baesjou, F. Budzelaar, M. Delden, S. Roosendaal, L. Stofmeel, A. Verschueren, J. Glabbeek, J. Osenga, and R. Schuurbiers, "Novel concept for full color electronic paper," *J. Soc. Inf. Disp.* **17**, 383–388 (2009).
 10. J.-S. Yeo, Z.-L. Zhou, T. Emery, G. Combs, V. Korthuis, J. Mabeck, R. Hoffman, T. Koch, and D. Henze, "Novel flexible reflective color media integrated with transparent oxide TFT backplane," *SID Symp. Digest of Tech. Papers* **41**, 1041–1044 (2010).
 11. J.-S. Yeo, Z.-L. Zhou, J. Mabeck, G. Combs, V. Korthuis, R. Hoffman, B. Benson, T. Koch, and D. Henze, "Novel flexible reflective color media with electronic inks," *J. Soc. Inf. Disp.* **12**, 5–10 (2010).
 12. T. Koch, J.-S. Yeo, J. Mabeck, R. Hoffman, B. Benson, G. Combs, V. Korthuis, Z. Zhou, and D. Henze, "Reflective electronic media with print-like color," in *Proceedings in NIP 27 and Digital Fabrication (IS&T2011)*.
 13. M. Goulding, L. Farrand, A. Smith, N. Greinert, H. Wilson, C. Topping, R. Kemp, E. Markham, M. James, J. Canisius, D. Walker, R. Vidal, S. Khoukh, S. Lee, and H. Lee, "Dyed Polymeric microparticles for color rendering in electrophoretic displays," *SID Symp. Digest of Tech. Papers* **41**, 564–567, (2010).
 14. S. Yang, M. Hagedon, and J. Heikenfeld, "Light out coupling for reflective displays: Simple geometrical model MATLAB simulation and experimental validation," *J. Disp. Technol.* **7**, 473–477 (2011).
 15. C. G. Granqvist, "Electrochromism and smart window design," *Solid State Ion* **53**, 479–489 (1992).
 16. S. Park and J. Hong, "Polymer dispersed liquid crystal film for variable transparency glazing," *Thin Solid Films* **517**, 3183–3186 (2009).

Reprinted from
Applied Optics